UNIVERSITY OF PARDUBICE

FAKULTY OF CHEMICAL TECHNOLOGY

Institute of Environmental and Chemical Engineering

Ing. Pavlína Kelíšková

Screen-printed sensors with boron-doped diamond electrode in electroanalysis of biologically active substances

Theses of the Doctoral Dissertation

Pardubice 2024

Study program: **Chemical and Process Engineering**

Study field: **Environmental Engineering**

Author: **Ing. Pavlína Kelíšková**

Supervisor: **doc. Ing. Renáta Šelešovská, Ph.D.**

Year of the defense: 2024

Reference
KELÍŠKOVÁ, Pavlína, Screen-printed sensors with boron-doped diamond electrode in electroanalysis of biologically active substances. Pardubice, 2024. Dissertation thesis (Ph.D.). University of Pardubice, Faculty of chemical technology, Institute of Environmental and Chemical Engineering, Supervisor doc. Ing. Renáta Šelešovská, Ph.D.

Abstract
This dissertation thesis deals with the development and optimization of electroanalytical methods using perspective screen-printed sensors for the determination of environmentally and pharmaceutically important substances. Attention was first devoted to the study and description of the electrochemical behavior of the drug guaifenesin and the pesticides cyprodinil and fludioxonil on a boron-doped diamond electrode (BDDE). After that, voltammetric methods were developed for their determination, when printed sensors with a working electrode from BDD were also applied. The basic strengths of these sensors were used, *i.e.*, analysis of small sample volumes and easy incorporation into electrochemical detectors in flow injection analysis. In order to increase the sensitivity of the determination of the studied analytes, new printed sensors with a structured surface were tested. Part of the study was their electrochemical characterization.

Abstrakt
Tato disertační práce se zabývá vývojem a optimalizací elektroanalytických metod s využitím perspektivních sítotiskových senzorů pro stanovení environmentálně a farmaceuticky významných látek. Pozornost byla věnována nejprve studiu a popisu elektrochemického chování léčiva guaifenesinu a pesticidů cyprodinilu a fludioxonilu na borem dopované diamantové elektrodě (BDDE). Poté byly vyvinuty voltametrické metody pro jejich stanovení, kdy byly aplikovány rovněž tištěné senzory s pracovní elektrodou z BDD. Byly využity základní přednosti těchto senzorů, tedy analýza malých objemů vzorků a snadná inkorporace do průtokových elektrochemických detektorů v průtokové injekční analýze. Za účelem zvýšení citlivosti stanovení studovaných analytů byly testovány nové tištěné senzory se strukturovaným povrchem. Součástí studie byla jejich elektrochemická charakterizace.

Keywords
Screen-printed sensors, boron-doped diamond electrode, structured surface, voltammetry, flow injection analysis with electrochemical detection, guaifenesin, cyprodinil, fludioxonil.

Klíčová slova
Sítotiskový senzor, borem dopovaná diamantová elektroda, strukturovaný povrch, voltametrie, průtoková injekční analýza s elektrochemickou detekcí, guaifenesin, cyprodinil, fludioxonil.

Table of Contents

Introduction

Electroanalytical methods are valuable tools in chemical analysis, recognized for their high sensitivity, precision, and broad applicability. These methods enable the quantification or identification of target analytes based on electrochemical principles. Since the development of polarography by Professor Jaroslav Heyrovský in 1922, for which he received the Nobel Prize in 1959, polarography and the derived voltammetry have become widely used, particularly in the Czech Republic, due to their traditional roots [1]. Voltammetry, a technique evolved from polarography, has seen significant advancement over the past 90 years, with numerous instrumental designs and techniques, such as pulse and stripping methods, expanding the analytical range. These methods now cover applications from trace heavy metal detection to the analysis of biologically active substances, including pesticides, drugs, and their metabolites. The choice of electrode material differentiates the methods [2].

Electroanalytical methods are based on an electrochemical cell, typically consisting of at least a working (polarizable) electrode and a reference (non-polarizable) electrode immersed in an electrolyte solution [3]. Common working electrodes include mercury, metals (*e.g.*, Au, Ag, Pt), and carbon-based electrodes, while reference electrodes, such as silver chloride and saturated calomel electrodes, help stabilize the cell's potential. More often, a three-electrode arrangement is used, adding an auxiliary electrode (typically platinum or carbon), allowing precise control over the working electrode's potential. Voltammetry measures current (I) as a function of the working electrode potential (E), which is applied by an external source and varies over time [5, 6]. This current response reflects the reduction or oxidation of the analyte, and results in a characteristic I-E curve (polarization curve), with the supporting electrolyte ensuring conductivity and constant ionic strength, usually selected to cover a wide potential range [4].

Over the years, various voltammetric methods have been developed, including direct current voltammetry (DCV), cyclic voltammetry (CV), differential pulse voltammetry (DPV), and stripping voltammetry (SV), with each method offering unique potential applications based on analyte properties and experimental goals. Recently, the development of new electrode materials aims to replace mercury and offer improved sensitivity, selectivity, or miniaturization. Carbon electrodes are highly versatile, allowing modifications via dopants, films, pastes, or modern nanomaterials applied by mechanical, physical, or chemical means [3].

Miniaturization and portability have become prominent in analytical chemistry, driven by the demand for field monitoring and point-of-care testing (POCT) in healthcare, food safety, and environmental monitoring. The miniaturization of electroanalytical methods, which includes sensors and detection systems, offers practical solutions due to ease of use, precision, high sensitivity, and rapid analysis, making them highly suitable for various real-world applications [5].

1. Theoretical part

1.1 Working electrodes

Working electrodes form an essential part of voltammetric experiments, their quality and selection significantly influence the measurement and interpretation of data. They must be chemically and mechanically stable, have high electrical conductivity, and sufficient reactivity. It is essential to consider the specific properties of the investigated system and the experimental requirements when selecting an electrode. Different types of electrodes, such as mercury, carbon, or printed electrodes, offer various advantages and disadvantages. Therefore, the correct choice is crucial for achieving accurate results.

1.2 Boron-doped diamond electrode

The boron-doped diamond electrode (BDDE) is a focal point of this dissertation. Diamond electrodes emerged in electrochemistry in 1983 when Japanese researchers modified diamond surfaces using gases like argon and nitrogen, as well as zinc and oxygen [6]. The foundation for their research was laid in 1962 with the development of chemical vapor deposition (CVD) methods for synthesizing diamonds [7]. The Japanese team improved this process by activating gas phases with hot filaments (HF) [8] and microwaves (MW) [9], enabling the synthesis of high-quality films. The unique properties of diamonds, such as hardness and chemical stability, make them attractive electrode materials, particularly when doped with other elements, most commonly boron. BDDE exhibits a wide potential window (approximately −1.5 V to 2.0 V in 0.1 M H2SO4), low noise, and a paraffinic surface, reducing adsorption issues and enhancing stability in flow systems [10].

BDDEs are synthesized via CVD using methane for carbon, hydrogen, and diborane or trimethylboron as boron sources. Their properties are influenced by various factors, particularly dopant concentration, typically ranging from 10^{17} to 10^{21} atoms of boron per cm^3 of diamond film [11]. The B/C ratio in the gas phase during deposition can vary from 500 to 15,000 ppm [10]. New preparation methods, including the use of liquid boron sources, have been developed, offering improved safety and growth rates for highly doped diamond layers [12]. BDDEs find extensive applications in monitoring and detecting inorganic and organic compounds, including pesticides and pharmaceuticals, vital for environmental and health protection [13–15].

Despite their advantages, studies are exploring surface modifications of BDDEs to enhance sensitivity and selectivity through various techniques, including chemical or electrochemical methods [16]. Common modifiers include metal nanoparticles [17] as well as organic molecules or biomolecules [18]. A distinct category includes structured or porous BDDEs, which enhance sensitivity and detection limits through various morphological changes achieved via etching, laser treatment, or deposition on porous substrates [19].

1.3 Screen printed sensors

A significant trend in contemporary analytical chemistry is the miniaturization and transfer of detection techniques to field settings or patient care. One solution in electroanalysis is the development of printed sensors combined with miniaturized potentiostats. These sensors are advantageous due to their simplicity, cost-effectiveness, and ability to analyze small sample volumes [20]. SPE has diverse applications, suitable

for classic three-electrode setups and compact designs for portable analyzers, facilitating sample volume analysis in the microliter range. This approach enables use in POCT (poin-of-care-testing) and environmental monitoring [21]. Produced via thick film technology, primarily screen printing, these sensors utilize carbon ink for its low cost and chemical inertness [22]. Recent advancements in nanotechnology have led to the use of metallic nanomaterials, such as Au and Ag nanoparticles, as printable conductive materials [23]. SPE can be manufactured in various shapes and surface modifications, allowing for configurations ranging from standalone working electrodes to complex systems with multiple electrode types for simultaneous analysis. SP/BDDE combines the benefits of disposable printed sensors, such as custom design, low costs, and easy mass production, with the excellent electrochemical properties of BDDE, including a wide potential window, low background currents, chemical resistance, and resistance to passivation.

This work utilized printed sensors with boron-doped diamond electrodes (SP/BDDE), developed in collaboration with the Slovak Diamond Grou. They combine the benefits of disposable sensors with the excellent electrochemical properties of BDDE, including low background currents and resistance to passivation [24].

1.4 Studied substances

1.4.1 Guaifenesin

Guaifenesin (GFE, Fig. 1A, CAS: 93-14-1) is a compound originally derived from the guaiac tree and was first synthesized in 1912. It has been used to treat respiratory conditions since the 19th century and was approved by the FDA for OTC use in 1989 [24]. GFE acts primarily as an expectorant for chronic respiratory diseases and is also classified as a central muscle relaxant, reducing skeletal muscle tension [26–28]. Considering the frequent use of this substance, it is necessary to have simple, fast, and sensitive methods for its determination available, both in pharmaceutical preparation and biological samples. The usually used instrumental techniques certainly allow for precise, sensitive, and selective determination of GFE in various types of samples with complex matrices. However, they are often quite demanding in terms of instrumentation and require complex sample preparation procedures before analysis.

Several studies have documented methods for GFE determination, predominantly using high-performance liquid chromatography (HPLC) with diode array detection (DAD) and mass spectrometry (MS) [29–35]. Other techniques include gas chromatography (GC) and spectrophotometric methods [36,37]. Despite the accuracy of these methods, they often require complex sample preparation. Electroanalytical methods offer simpler alternatives. Various modified carbon electrodes, such as glassy carbon, carbon paste, and screen-printed carbon electrodes, have been frequently used for GFE analysis. Their modifications include nanomaterials like nanoparticles, polymers, and carbon nanotubes [37–39]. The preparation of these sensors is quite complicated, which can lead to poorer repeatability. BDDE or SP/BDDE, respectively, could represent a simple and sufficiently sensitive alternative.

1.4.2 Fludioxonil

Fludioxonil (FLU, Fig. 1B, CAS: 131341-86-1) is a broad-spectrum fungicide used primarily for protecting stored seeds, fruits, and vegetables. Its application has increased

significantly in recent years, now used on over 900 crop types [38]. FLU's mechanism of action, still under investigation, likely involves disrupting cellular metabolism, like to pyrrolnitrin, leading to increased reactive oxygen species (ROS) that damage cell structures [39,40]. FLU is primarily introduced into the environment through commercial fungicides, exhibiting low mobility but accumulate in soil and sediments, with degradation half-lives of 200-300 days [40]. While it generally poses low acute toxicity to most organisms, it can disrupt hormonal balance in sensitive species, raising concerns in developed countries regarding pesticide pollution [41,42].

Detection of FLU in various matrices such as fruits, vegetables, and soil is commonly performed using chromatographic methods coupled with mass spectrometry (GC-MS) [43–46]. Immunochemical detection was also described [46]. Only one study focused on the electrochemical analysis of FLU using a silver amalgam Hg(Ag)FE film electrode with a detection limit of 5.8×10^{-7} mol L^{-1} was mentioned in the literature [48].

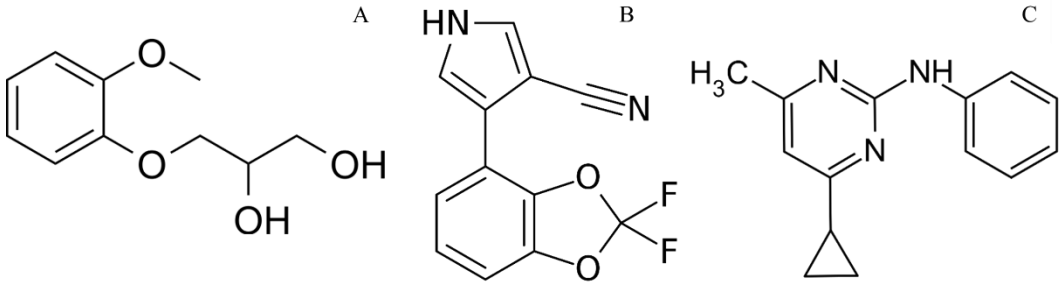

Figure 1: *Structural formula of guaifenesin (A), cyprodinil (B), and fludioxonil (C).*

1.4.3 Cyprodinil

Cyprodinil (CPD, Fig. 1C, CAS: 121552-61-2) is a broad-spectrum fungicide used in agriculture to protect crops from pathogens. It belongs to the anilinopyrimidines group, which inhibits methionine biosynthesis and enzyme secretion in fungi [49,50]. Three active ingredients are available: cyprodinil, mepanipyrim, and pyrimethanil, differing by their 4-position substituents on the pyrimidine ring [49]. CPD is resistant to metabolic changes and is applied as an aqueous solution or emulsion on plant leaves. It enters the environment primarily through rainfall, posing risks to aquatic organisms. The EPA classifies it as having low toxicity for humans and most animals but moderate toxicity for fish and high toxicity for aquatic invertebrates [51–53].

Most studies focus on chromatographic methods for detecting anilinopyrimidines, primarily using solid-phase microextraction (SPME) and liquid-liquid extraction (LLE) [49,54]. For example, SPME has been used to analyze CPD in blueberries with limits of detection (LOD) of 1.2 μg/kg [55]. HPLC methods often utilize solvent extraction, with recent developments allowing for the detection of CPD in fruits and vegetables at LODs ≤ 0.4 μg/kg [44]. Immunochemical methods, particularly ELISA, have been applied for rapid pesticide analysis in food matrices [56,57]. One study on CPD's electrochemical behavior used MWCNT/CPE electrodes, reporting a quasi-reversible oxidation peak at 1.2 V, achieving an LOD of 0.076 mg/L for water and juice samples [58].

2. Experimental part

2.1 Chemicals

All chemicals used for preparing the supporting electrolytes, standard, and other stock solutions were of analytical grade (p.a.). Standard solutions of GFE, FLU, and CPD (Sigma-Aldrich, CZ) were initially prepared at a concentration of 1.0×10^{-3} mol L^{-1} by dissolving in acetonitrile (Honeywell, CZ) under ultrasound. The solutions were stored in a refrigerator (4 °C) away from light. Lower concentration solutions were freshly prepared daily by diluting with the electrolyte. The Britton-Robinson buffer (BRB) was made by mixing the acidic and alkaline components. The acidic component was prepared from stock acids: 99.8% H_3BO_3, 85% H_3PO_4, and 99.8% CH_3COOH (Ing. Petr Švec – PENTA s.r.o., CZ), resulting in an acid concentration of 0.04 mol L^{-1}. The alkaline component consisted of 0.2 mol L^{-1} NaOH (PENTA). Further supporting electrolytes were prepared from diluted solutions of 96% H_2SO_4, 85% H_3PO_4, 65% HNO_3, 99% CH_3COOH, and 35% HCl (PENTA). For interference studies, solutions of selected pesticides were prepared at a concentration of 1.0×10^{-3} mol L^{-1}, including glyphosate, difenoconazole, triticonazole, cyprodinil, paclobutrazol, tebuconazole, azoxystrobin, benalaxyl, metalaxyl, imidacloprid, cyproconazole, epoxiconazole, azoxystrobin, dicamba, fludioxonil, and folpet (Sigma-Aldrich, CZ).

As real samples, pharmaceutical products analyzed for GFE included Stoptussin 20MG (declared 20 mg/mL GFE, Teva Pharmaceutical Industries, CZ), Guajacuran 200MG (200 mg/tablet, Zentiva Group, CZ), and Biochemical Control Serum Human I (Biosystems S.A., ES). The solutions were prepared to achieve a resulting concentration of GFE of 1.0×10^{-3} mol L^{-1} (based on the declared content). For CPD, the commercially available pesticide product CHORUS 50WG was used, containing 500 g/kg of CPD (Syngenta Crop Protection AG, CH), along with the mixture product Switch, which contains 375 g/kg of CPD (37.5% w/w) and 250 g/kg of FLU (25% w/w) (AgroBio, CZ). River water was analyzed from the Loučná River near Dašice (Pardubice Region, CZ), and well water was collected in Slatiňany (Pardubice Region, CZ).

For the electrochemical characterization of the sensors, a 0.1 mol L^{-1} KCl solution was prepared by dissolving the powder (PENTA) in distilled water. Stock solutions of 2.5 mmol L^{-1} $K_3[Fe(CN)_6]$ and $[Ru(NH_3)_6]Cl_3$ (> 99%, Sigma-Aldrich, CZ) were prepared by dissolving in 0.1 mol L^{-1} KCl. Infrared spectroelectrochemistry was performed in anhydrous acetonitrile (water < 0.001%) using tetrabutylammonium hexafluorophosphate (NBu_4PF_6) as the indifferent electrolyte (both Sigma Aldrich, CZ).

2.2 Instrumentation

Voltammetric measurements were conducted using the Autolab PGSTAT12 potentiostat (Metrohm Autolab, NL) with Nova 2.1.5 software, connected to an electrochemical impedance spectroscopy (EIS) module FRA32M. In a classic three-electrode setup, a boron-doped diamond electrode (BDDE, Fig. 2A) served as the working electrode (WE) (BioLogic, France, active surface 7.07 mm^2, inner diameter 3 mm, B/C ratio 1000 ppm). A saturated silver/silver chloride electrode (Ag/AgCl/KCl sat.) was used as the reference electrode (RE), and a platinum wire served as the counter electrode (CE) (both Monokrystaly, CZ). SP/BDDE sensors (Fig. 2B, Slovak Diamond Group, Slovak University of Technology (STU) in Bratislava, SK) were used, with their preparation

described in an earlier work from our laboratory [24]. These sensors consisted of WE and CE made from BDD, produced using a large-area linear antenna microwave chemical vapor deposition (LA-MWCVD) system, and a quasi-RE of Ag/AgCl. Three types of sensors with different WE areas were utilized, labeled as 1-3: 1-SP/BDDE (0.785 mm^2, 1 mm diameter), 2-SP/BDDE (3.14 mm^2, 2 mm), and 3-SP/BDDE (7.07 mm^2, 3 mm).

Additionally, sensors with a structured BDDE surface (sSP/BDDE, Fig. 2C) were tested, having a WE diameter of 3 mm. The substrate area of WE was modified using a laser to create a grid with defined dimensions, and individual grooves were deepened by repeating the laser scans. The structures were designated as follows: 5×15, 5×20, 5×25, and 10×15, 10×20, 10×25, where the first value (5 and 10) represents the number of repeated laser scans and the second value (15, 20, and 25) indicates the grid dimensions in μm. BDD was deposited on this modified substrate using LA-MWCVD. The configuration of the entire electrochemical cell and the parameters for CE and RE were the same as those for 3-SP/BDDE.

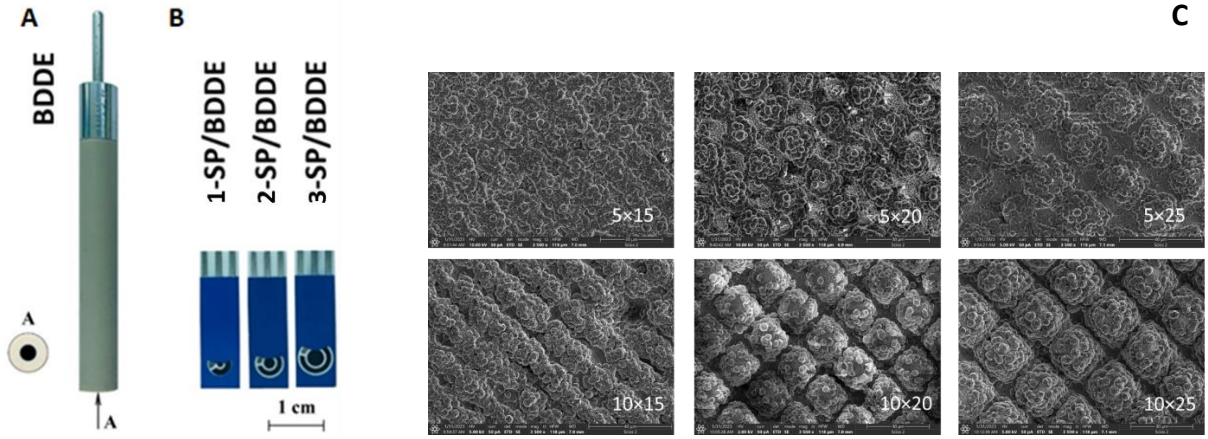

***Figure 2**: Sensors used in this work: (A) commercially available BDDE, (B) printed sensors with varying sizes of (WE) area, and (C) surface of sSP/BDDE.*

Flow injection analysis with electrochemical detection (FIA-ED) was assembled from a programmable pump (Protea, USA), a 50 mL plastic syringe (Steriwund, PL), a chromatographic six-port injection valve (Supelco, USA) with an injection loop, tubing, and a flow cell printed on a 3D printer (STU in Bratislava, SK) with an inserted SP/BDDE sensor. The injection loop was filled with the sample using a 5.0 mL syringe.

For the pre-concentration of samples, a solid-phase extraction setup was used, consisting of a Visiprep SPE Vacuum Manifold (Merck, DE) with Chromabond C18ec columns (Macherey-Nagel, DE). A KNF Laboport® mini pump (KFN Group, DE) was used to create a vacuum. A rotary vacuum evaporator, Laborota 4001 (Heidolph, DE), was employed for the evaporation of eluates.

For comparative HPLC analysis of model and real samples, an Agilent 1260 Infinity II Prime LC system (Agilent, USA) with a DAD detector was utilized. Absorption spectra for spectroelectrochemical measurements were obtained using a Nicolet iS50 FTIR spectrometer (Fourier-transform infrared spectrometer) equipped with a KBr beam splitter. Additional laboratory equipment included a pH meter (Accument AB 150, Fisher Scientific, CZ), analytical balances (Denver Instrument, USA), and an ultrasonic bath (Bandelin SONOREX, Schalltec GmbH, DE).

2.3 Procedures

BDDE was activated by performing 20 cyclic voltammograms in a 1.0 mol L^{-1} H_2SO_4 from −1.5 V to +2.2 V at a scan rate of 0.1 V s^{-1}. There was no surface passivation between measurements, eliminating the need for repeated activation. For SP/BDDE, electrode contacts were cleaned with an eraser, and the working electrode was activated using cyclic voltammetry (CV, 10 cycles) in 1.0 mol L^{-1} H_2SO_4 The potential range was from −0.5 V to +2.0 V. The study of the voltammetric behavior of GFE, CPD, and FLU was conducted using CV (E_{in} = –1.5 V, E_{switch} = 2.2 V, v = 0.1 V s^{-1}). The influence of the scan rate was tested within the range from 0.025 to 0.2 V s^{-1}.

For the development of methods for determining of the analytes, differential pulse voltammetry (DPV) and square-wave voltammetry (SWV) were tested. First, a suitable supporting electrolyte was chosen, and then the parameters were optimized: scan rate (v), pulse amplitude (A), and modulation time (t) for DPV, and scan rate (v), pulse amplitude (A), and frequency (f) for SWV. The resulting parameters for individual analytes and methods are summarized in Table 1.

Table 1: Optimized parameters of DPV and SWV for studied substances.

Analyte	Method	Electrolyte	v [V s^{-1}]	A [V]	t [ms]	f [Hz]
GFE	DPV	BRB pH 2	0.04	0.04	20	---
	SWV	BRB pH 2	0.04	0.03	---	20
CPD	DPV	1M CH_3COOH	0.03	0.04	40	---
	SWV	1M CH_3COOH	0.03	0.03	---	30
FLU	DPV	0.1M H_3PO_4	0.05	0.05	50	---
	SWV	0.1M H_3PO_4	0.05	0.05	---	10

CV was also used to characterize sSP/BDDE using redox markers $[Ru(NH_3)_6]^{2+/3+}$ and $[Fe(CN)_6]^{4-/3}$. Cyclic voltammograms were recorded over a potential range from –0.8 to +0.3 V ($[Ru(NH_3)_6]^{2+/3+}$) and from –0.8 to +0.8 V ($[Fe(CN)_6]^{4-/3}$) with scan rate of 0.1 V s^{-1}. Dependencies on the polarization rate were recorded over the range of from 0.025 to 0.2 V s^{-1}. The concentrations of the markers in these experiments were 2.5 mmol L^{-1}. During the characterization of sSP/BDDE using EIS, measurements were taken over a f range from 10 kHz to 1,0 Hz with a pulse amplitude of 10 mV. The redox markers were 2.5 mmol L^{-1} solutions of $[Fe(CN)_6]^{4-/3-}$ and $[Ru(NH_3)_6]^{2+/3+}$ in 0,1 mol L^{-1} KCl. The values of individual elements in the electrical equivalent circuits were calculated using FRA simulation in Metrohm NOVA software version 2.1.5.

In case of FIA-ED, the system was flushed with the mobile phase, *i.e.*, the supporting electrolyte selected for the voltammetric analysis of the respective analyte. This also filled the entire 50 mL injection syringe; it was BRB (pH 2) for GFE, and 1,0 mol L^{-1} CH_3COOH for CPD. The basic parameters of FIA-ED were optimized as follows: CPD – flow rate of the mobile phase (F_m) = 1,5 mL min^{-1}, volume of sample (V_{inj}) = 25 µL and potential of detection (E_{det}) = 0,9 V; GFE – F_m = 1 mL min^{-1}, V_{inj} = 50 µL and E_{det} = 1,4 V. The dosing loop was washed and filled with the sample using a 5 mL plastic syringe. The sample dosing was performed manually. After measurement, the FIA system was rinsed with distilled water and acetonitrile.

GFE was determined in pharmaceutical preparations and serum. A Guajacuran tablet was crushed, transferred to a 100 mL volumetric flask, and diluted with distilled

water. The flask was placed in an ultrasonic bath for 15 minutes. For Stoptussin syrup, 1 mL was measured into a 100 mL flask and diluted similarly. Both samples were analyzed using DPV and FIA-ED applying calibration curve method. For serum analysis, SP/BDDE was used, and DPV analysis was conducted in 50 μL droplets without addition of supporting electrolyte. Analysis was evaluated by calibration curve method again.

Pesticides FLU and CPD were analyzed in natural waters and pesticide preparations. Water samples from the Loučná River and Slatiňany well were filtered and enriched with standard solutions of the respective pesticides (FLU at 1.0×10^{-8} mol L^{-1} and CPD at 5.0×10^{-8} mol L^{-1}). CPD was analyzed directly using DPV and the standard addition method, while FLU required concentration enrichment through solid-phase extraction (SPE) when 0.5 L of water was extracted on five C18 solid-phase SPE columns, eluted with acetonitrile and evaporated. The residue was dissolved in acetonitrile, diluted with electrolyte, and analyzed by SWV. DPV and FIA-ED were subsequently used to analyze two fungicide products Chorus 50WG and Switch. Solutions of Chorus and Switch were prepared by dissolving 45.1 mg and 60.1 mg of each product in 1.0 L of distilled water with 1.0 mL of 99% acetic acid (CH_3COOH) added. The resulting CPD concentration in the solutions was approximately 1.0×10^{-4} mol L^{-1}, based on the manufacturer-reported CPD content. DPV analysis was conducted in 1.0 mol L^{-1} CH_3COOH using the standard addition method. FIA-ED analysis of both fungicides was also performed in 1.0 mol L^{-1} CH_3COOH using a calibration curve method.

In case of mechanism proposal for GFE electrochemical oxidation, calculations were based on Density Functional Theory (DFT). Were performed to study the spatial arrangement of frontier orbitals, atomic charges, and bond orders. These calculations used the B3LYP functional and 6-31G* basis set in Spartan '14 software (Wavefunction, Inc., USA) for molecules optimized geometrically in a vacuum. Infrared spectra were calculated using DFT with the EDF2 functional and the 6-31G** basis set. Infrared spectroelectrochemical measurements were conducted in a thin-layer optically transparent three-electrode cell with CaF2 windows, allowing IR spectra observation over the range of 4000 to 650 cm^{-1}, and used Ag/AgCl as a quasi-reference electrode and two platinum grid electrodes as working and auxiliary electrodes.

Samples containing GFE and CPD were analyzed also via HPLC/DAD. Analyses were performed on a Macherey-Nagel EC 250/4 Nucleosil 120-5 C18 column (4×250 mm, 5 μm particle size) at 25 °C. For GFE, the mobile phase was CH_3CN/H_2O (40/60, v/v) with a flow rate of 0.5 mL min^{-1}, injection volume of 30 μL, and DAD detector wavelength at 226 nm. For CPD, the mobile phase was CH_3CN/H_2O (80/20, v/v) with 0.1% formic acid, flow rate of 1.0 mL min^{-1}, injection volume of 10 μL, and wavelength at 264 nm. Analysis times were 7 minutes for GFE and 5 minutes for CPD.

Data processing and calculations were provided by Software OriginPro 9 (Origin Lab Corporation, USA) was used to calculate calibration curve parameters and confidence intervals. LOD was calculated as three times, and LOQ as ten times, the standard deviation of the intercept, divided by the slope of the peak height *vs.* concentration linear dependence.

3. Result and discussion

3.1 Guaifenesin

3.1.1 Electrochemical Behavior of Guaifenesin

Electrochemical behavior of GFE was studied using both BDDE and 3-SP/BDDE. CV revealed that GFE (100 µmol L^{-1}) produced a well-defined oxidation peak at around +1.0 V on 3-SP/BDDE in BRB (pH 2.0) and a second indistinct signal at +1.1 V (Fig. 3A). No significant reduction peak was observed, indicating an irreversible reaction. A similar response was seen on BDDE, with a shift to more positive potentials. Subsequent experiments were focused on GFE's response in various pH. The voltammograms recorded in BRB (pH 2-12) and 0.1 mol L^{-1} H_2SO_4 are shown in Fig. 3B-D. The peak height (I_p) decreased with increasing pH, and the highest I_p was observed at pH 2. E_p shifted to less positive values with increasing pH, indicating the involvement of protons. Based on these findings, BRB (pH 2) was chosen as the electrolyte.

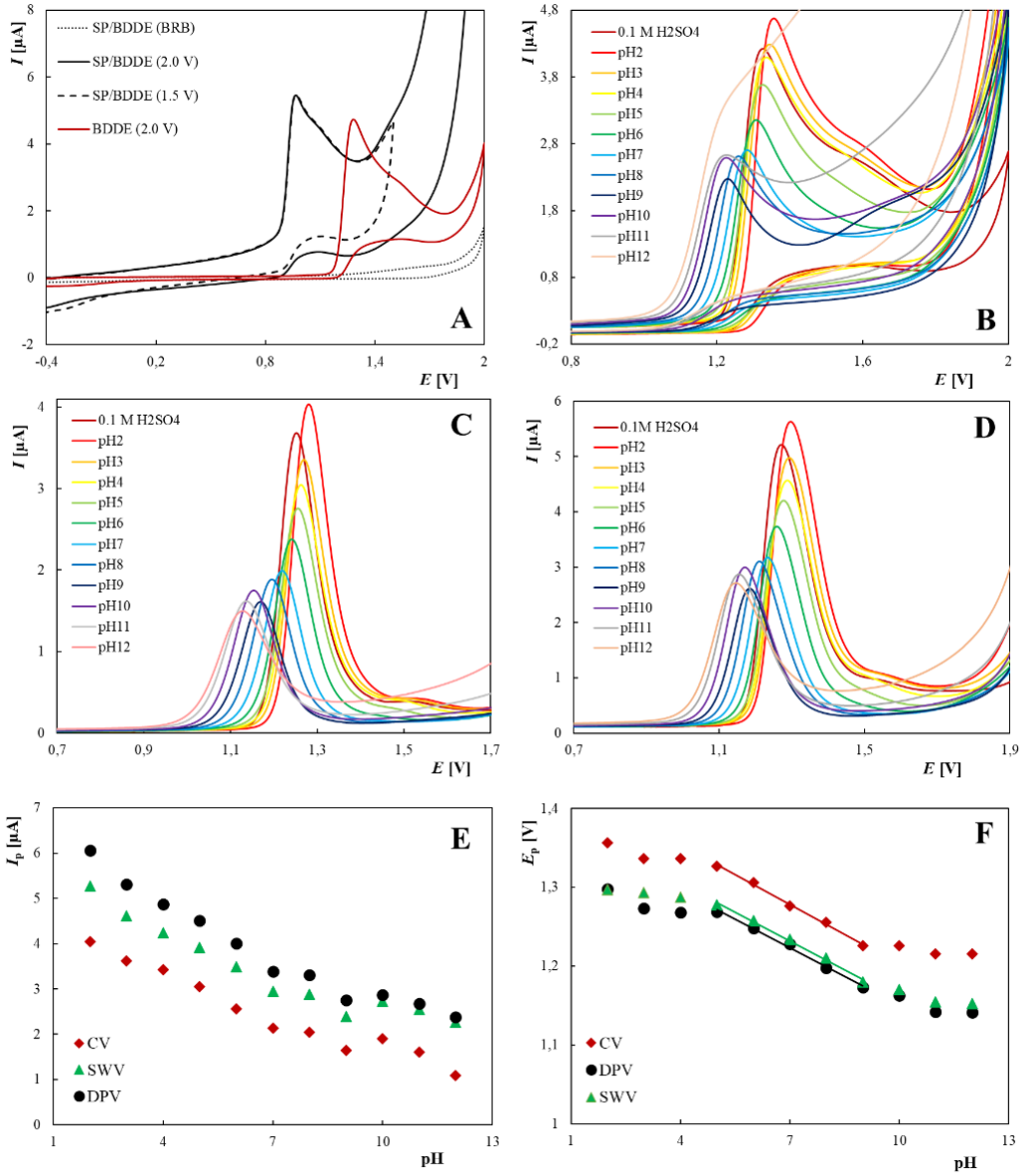

Figure 3: *CV voltammograms of GFE on BDDE and 3-SP/BDDE (A), CV (B), DPV (C) and SWV (D) voltammograms in dependence on pH and dependencies of I_p on pH (E) and E_p on pH (F) for BDDE.*

The voltammetric curves obtained in dependence on scan rate showed that I_p increases with increasing v, with the linear relationship of I_p to $v^{1/2}$ indicating a diffusion-controlled reaction. E_p also shifts to more positive potentials, confirming the irreversible nature of GFE's oxidation.

3.1.2 Mechanism of Electrochemical Oxidation of Guaifenesin

The results indicate that protons play a role in GFE oxidation. The shapes of cyclic voltammograms vary with pH, indicating multiple oxidation pathways depending on pH. However, the oxidation process is diffusion-controlled, allowing for the proposal of an overall reaction scheme. The $\delta E_p/\delta \log v$ value (0.044 V) for BDDE aligns with the ECE-DISP process rather than radical-radical dimerization. The dependence of E_p on concentration is not linear, indicating a more complex process.

In-situ IR spectroelectrochemistry was employed to obtain detailed information about the oxidation process (Fig. 4). The IR adsorption spectrum of GFE in acetonitrile with NBu_4PF_6 electrolyte showed reduced water absorption bands during oxidation, indicating water's involvement in GFE oxidation. Absorption bands of GFE also decreased, while new bands appeared, suggesting the formation of oxidation products. Calculations indicate that the active site in the molecule is located on the carbon atoms in the aromatic ring. During oxidation, the second hydroxyl group attacks the positively charged carbon, forming product P1. Further oxidation leads to the cleavage of the benzene ring, similar to mefenoxalon, which has a comparable structure to GFE. The order of the C1-C2 bond in the dihydroxylated intermediate was calculated to be 0.875. Hydroxyl groups were oxidized to oxo groups, confirmed by increased absorption in the carbonyl region. The oxidation of GFE leads to various final products due to its structure, especially the presence of the easily oxidizable ethylene glycol group, which was identified as product P3.

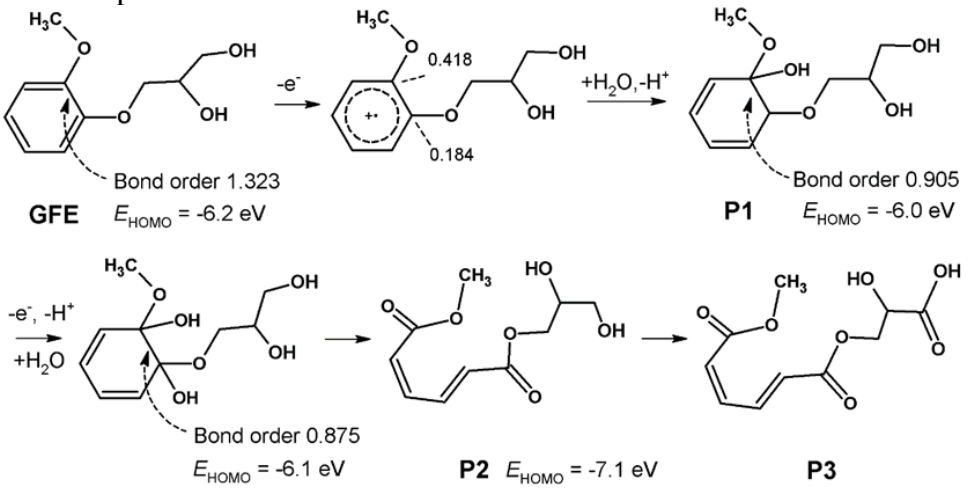

Figure 4: *Proposed oxidation mechanism of GFE.*

3.1.3 Development of the Voltammetric Method for Determining Guaifenesin

For developing the voltammetric method for GFE, DPV and SWV techniques were employed. A BRB (pH 2) was selected as electrolyte based on previous pH studies (Fig. 3). Parameters such as scan rate (v), pulse amplitude (A), and pulse width (t) for DPV, respectively frequency (f) for SWV, and BDDE surface pre-treatmen procedure were

optimized. Concentration dependencies of GFE from 10 to 50 µmol L^{-1} were measured using both sensors and both methods. DPV was preferred due to sharper peaks compared to SWV, with 3-SP/BDDE showing higher sensitivity (0.081±0.001) than BDDE. Using the newly developed DPV method, the linear dynamic range (LDR, Fig. 7), LOD, and LOQ were established. Results indicated better performance for 3-SP/BDDE with lower LOD (40 nmol L^{-1}) and wider LDR (0.1-155 µmol L^{-1}) compared to BDDE (Table 2).

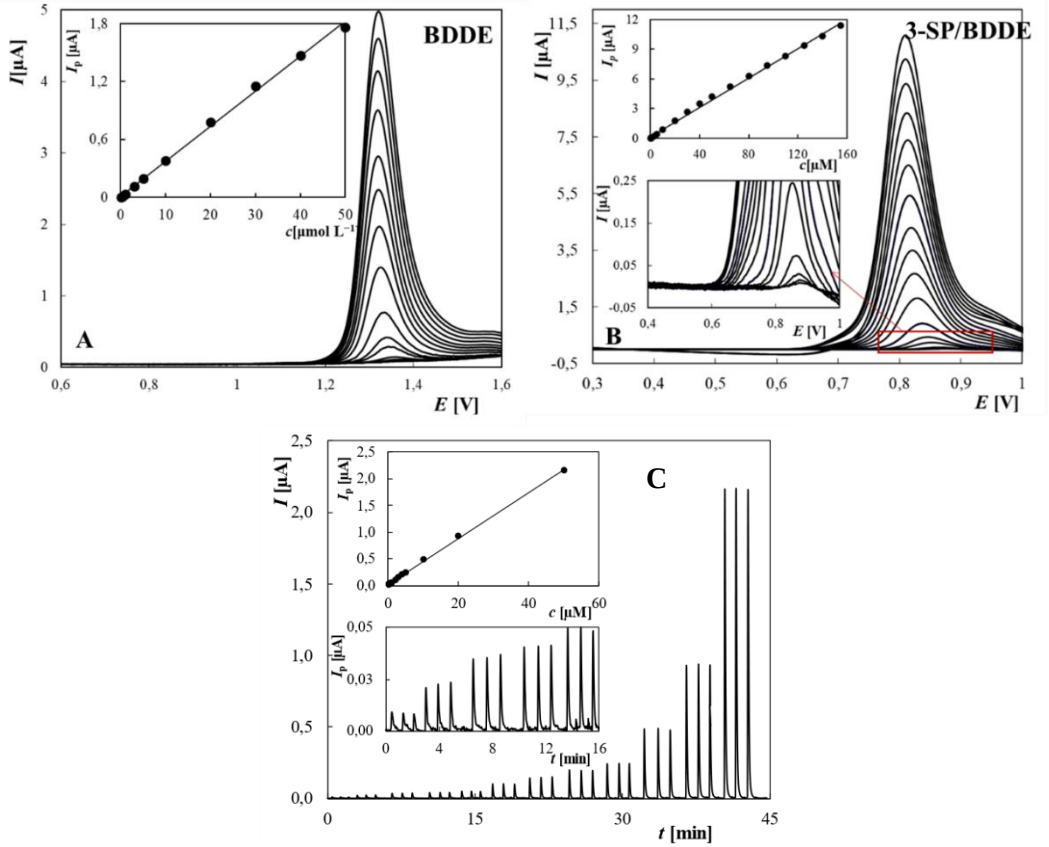

Figure 5: *DP voltammograms of GFE in dependence on c on BDDE (A) and 3-SP/BDDE (B), chronoamperogram of GFE recorded using FIA-ED in connection with 3-SP/BDDE.*

Table 2: Statistical parameters for GFE determination using the developed methods.

Method	Electrode	LOD [µmol L^{-1}]	LOQ [µmol L^{-1}]	LDR [µmol L^{-1}]
DPV	BDDE	0.091	0.30	0.1-80
DPV	3-SP/BDDE	0.041	0.14	0.1-155
FIA-ED	3-SP/BDDE	0.086	0.29	0.1-50

***** LOD and LOQ values calculated from concentration dependences in the range 0.1-5.0 µmol L^{-1}.

Printed sensors are advantageous for easy integration into flow systems. This work focused on developing a GFE determination method using FIA-ED with 3-SP/BDDE as the electrochemical detector. The optimization of parameters was the first step. Then the optimized method was applied to measure the concentration dependencies of GFE, with the LDR determined and LOD and LOQ values calculated. Fig. 5 presents an example of the resulting chronoamperogram for GFE concentrations ranging from 0.1 to 50 µmol L⁻1, representing the full LDR of this method. As shown in Table 2, the achieved LOD (0.086 µmol L⁻1) and LOQ (0.29 µmol L⁻1) values were comparable to those of DPV with BDDE and slightly higher than for DPV with 3-SP/BDDE.

To compare results with an independent method, HPLC/DAD was employed, optimizing parameters like wavelength (λ) and mobile phase composition. The optimal λ was 226 nm, with a mobile phase of 40% acetonitrile and 60% water. The linearity of the method was confirmed for GFE concentrations from 0.2 to 7.0 μmol L^{-1}. The dependence insert in Fig. 6 confirms that the peak area increases linearly within the specified range as a function of analyte concentration.

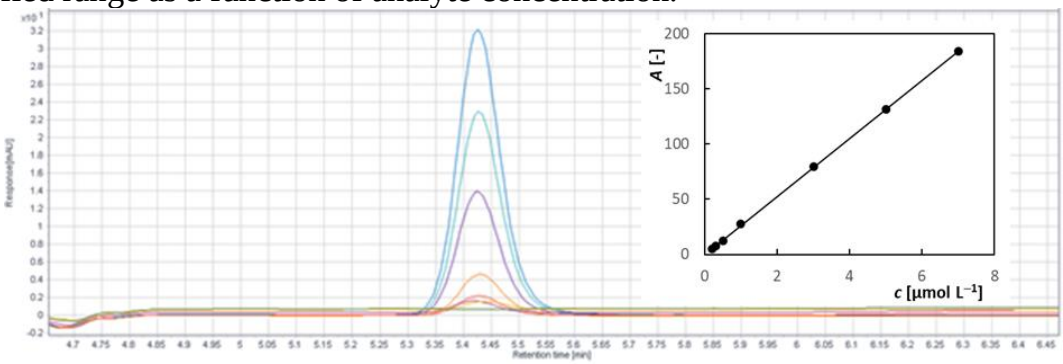

Figure 6: *Chromatograms of GFE obtained in dependence on c using HPLC/DAD.*

3.1.4 Analysis of Model Solutions and Real Samples

The validity of the proposed methods was confirmed through model solutions containing GFE at concentrations of 2.0 and 0.5 μmol L^{-1} in BRB (pH 2.0) using a calibration curve method (Fig. 7). Statistical parameters were calculated from five repeated analyses, summarized in Table 3, indicating that all proposed methods, including DPV with BDDE or SP/BDDE and FIA-ED, provided accurate and reproducible results in accordance with HPLC/DAD.

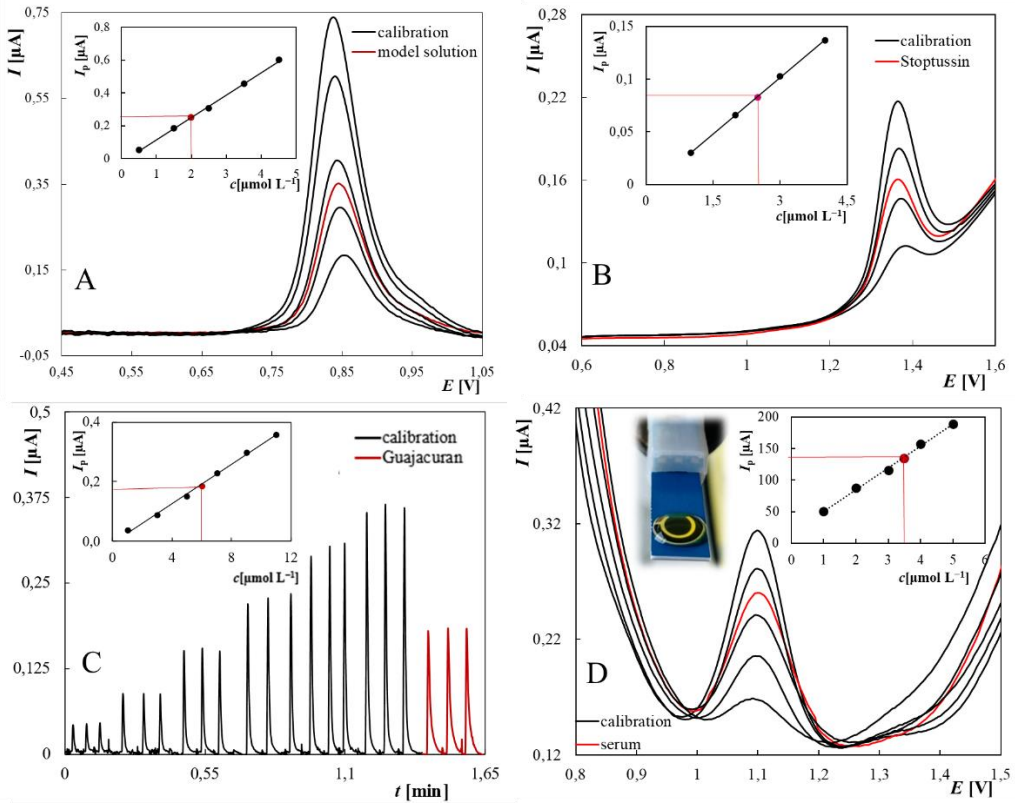

Figure 7: *DP voltammograms of model solution (A) and Stoptussin (B) analysis on 3-SP/BDDE, chronoamperograms of Guajacuran analysis using FIA-ED (C), and DP voltammograms of serum analysis in 50 μL drop on 3-SP/BDDE (D).*

Subsequently, the proposed methods were applied to analyze pharmaceutical products Guajacuran and Stoptussin, containing 200 mg of GFE per tablet and 20 mg mL^{-1} in syrup, respectively. The analysis examples for Stoptussin applying DPV with 3-SP/BDDE, and Guajacuran applying FIA-ED are shown in Figures 7B and C. The results in Table 3 were in good agreement with the declared GFE content in both types of samples. All developed methods can be successfully used for pharmaceutical analysis, with the advantage of FIA-ED and its suitability for automation and large sample series analysis. The effect of potential interfering substances investigated with regard to the application of the method in the analysis of biological samples was not significant except for the folic acid, barbituric acid, and ascorbic acid in a tenfold excess. Finally, the possibility of determining GFE in serum using DPV with 3-SP/BDDE was tested, applying a 50 μL droplet to the sensor without any sample preparation or electrolyte addition. The GFE concentration in serum was 3.5 μmol L^{-1}, corresponding to levels in patients taking GFE-based medications. The analysis yielded accurate and reproducible results demonstrating that the proposed method can be effectively applied to biological sample analysis without complicated preparation.

Table 3: Result of model solution and real samples analysis

Sample	**Method**	**Added [μmol L^{-1}]**	**Found [μmol L^{-1}]**	**Recovery [%]**	**RSD [%]**
Model solution	DPV, BDDE	2.0	2.001±0.012	99.3-101.0	0.6
		0.5	0.504±0.006	98.9-102.7	1.2
	DPV, 3-SP/BDDE	2.0	1.982±0.025	98.5-101.3	1.3
		0.5	0.489±0.015	96.3-104.8	3.0
	FIA-ED, 3-SP/BDDE	2.0	1.957±0.070	92.9-102.9	3.6
		0.5	0.494±0.019	95.5-105.4	3.8
	HPLC/DAD	2.0	2.024±0.043	98.2-103.9	2.1
		0.5	0.512±0.019	97.3-108.7	3.7
		Declared [mg Tbl^{-1}]	Found [mg Tbl^{-1}]	Recovery* [%]	RSD [%]
Guajacuran	DPV, BDDE	200	196.7±4.3	95.1-100.9	2.2
	DPV, 3-SP/BDDE	200	200.8±3.7	98.2-103.4	1.8
	FIA-ED, 3-SP/BDDE	200	195.9±8.2	94.5-104.4	3.8
	HPLC/DAD	200	199.0±9.7	90.5-105.1	4.9
		Declared [mg mL^{-1}]	Found [mg mL^{-1}]	Recovery* [%]	RSD [%]
Stoptussin	DPV, BDDE	20	20.025±0.423	98.3-102.8	2.1
	DPV, 3-SP/BDDE	20	19.995±0.237	98.6-101.7	1.2
	FIA-ED, 3-SP/BDDE	20	19.772±0.404	96.8-101.5	2.1
	HPLC/DAD	20	20.201±0.550	97.6-105.0	2.7
		Added [μmol L^{-1}]	Found [μmol L^{-1}]	Recovery [%]	RSD [%]
Serum	DPV, 3-SP/BDDE	3.5	3.488±0.109	95.0-103.6	3.2

* The values were related to the amount of active substance declared by the manufacturer.

3.2 Cyprodinil and Fludioxonil

3.2.1 Electrochemical Behavior of Fludioxonil and Cyprodinil

Cyclic voltammograms of CPD in 0.1 μmol L^{-1} CH_3COOH and FLU in 0.1 μmol L^{-1} H_3PO_4, both at a concentration of 100 μM, were recorded on BDDE as well as on SP/BDDEs with different surface area, converting current values to current densities (*j*) (Fig. 8). The voltammograms showed two anodic peaks for CPD $E_{p,1}$ = +1.4 V and $E_{p,2}$ = +1.7 V (BDDE) for CPD and $E_{p,1}$ = +1.5 V and $E_{p,2}$ = +2.1 V (BDDE) for FLU. The reaction for FLU was irreversible, while CPD exhibited a less pronounced cathodic peak at E_p = −0.2 V. Applying different reversal potentials indicated that with E_{switch} = +1.55 V, immediately after CPD's first anodic response, no cathodic peak was observed, indicating an irreversible first oxidation step for CPD. SPE showed higher peaks for CPD and FLU compared to BDDE, likely due to greater boron doping. Peaks for both analytes shifted to less positive potentials on SP/BDDE due to the quasi-RE used.

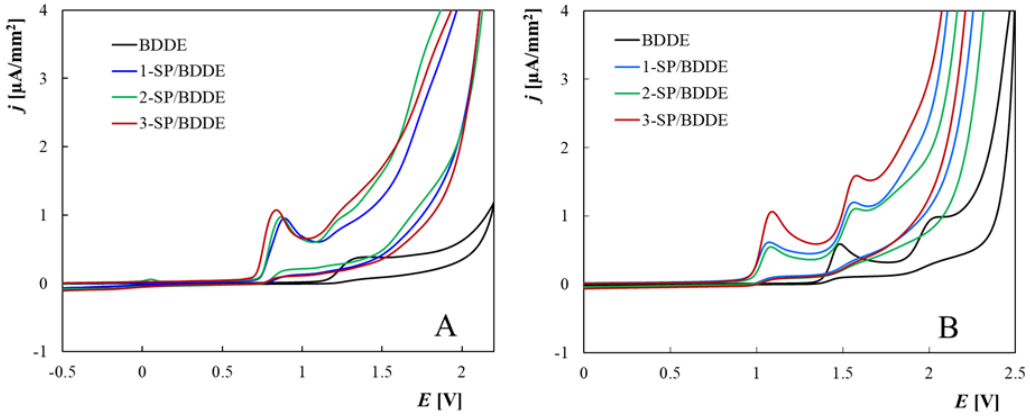

Figure 8: *Cyclic voltammograms of CPD (A) and FLU (B) recorded on BDDE and SP/BDDE.*

Studies of the effect of pH and the composition of the supporting electrolyte showed that 0.1 μmol L^{-1} CH_3COOH is a suitable medium for CPD and 0.1 μmol L^{-1} H_3PO_4 for FLU. Due to the dependence of j_p on the scan rate, diffusion was determined to be the controlling process for the reactions of both pesticides. In the case of CPD, the possible influence of adsorption was manifested in SPEs which became more pronounced with increasing area of sensors WE. The highest value of the slope of the logarithmic dependence of I_p on *v* (0.724±0.009) was recorded for 3-SP/BDDE. This effect may be related to the higher boron doping level, which brings with it an increase in the sp^2 carbon content in the BDD film which is more prone to adsorption than sp^3 carbon.

3.2.2 Development of the Voltammetric Method for Determination CPD and FLU

The development of methods for determination of CPD and FLU followed the same approach as described for GFE. Parameters for DPV and SWV were optimized using BDDE and various pre-treatment methods were tested. Comparison of DPV and SWV under optimized conditions revealed similar responses, with DPV chosen for CPD (Fig. 9A) due to better repeatability (RSD = 1.9%) compared to SWV (RSD = 6.27%). For FLU (Fig. 9C), SWV provided slightly higher sensitivity and repeatability (RSD = 1.1%). The experimentally determined LDR for CPD was 0.025-1.9 μmol L^{-1} (Fig. 9A) and for FLU was 0.5-50 μmol L^{-1} (Fig. 9D). Methods were successfully adapted for SP/BDDE (Fig. 9B for CPD), showing higher sensitivity than BDDE with decreasing

LOD values correlated with increasing WE area. The FIA-ED method was also developed for CPD, where the influence of the size of the WE of the SPE on the analytical parameters was tested. It was shown that the 1-SP/BDDE with the smallest WE area provided the highest sensitivity (Fig. 10A).

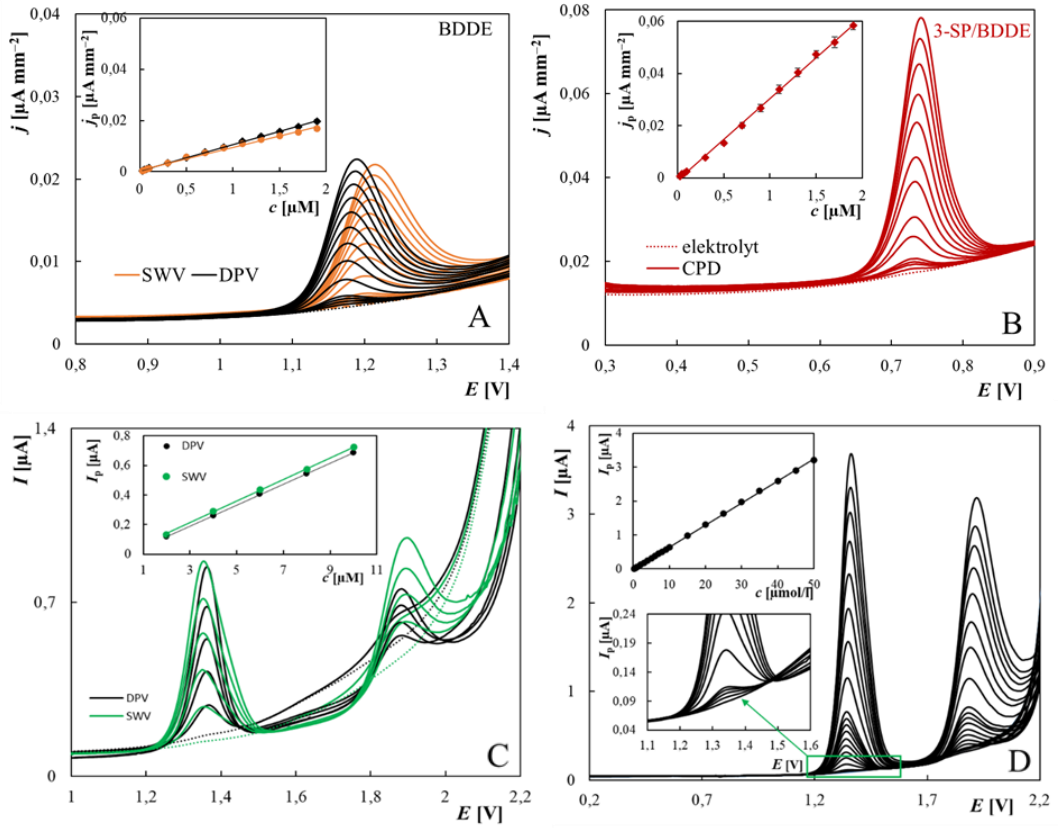

Figure 9: *DP and SW voltammograms of CPD recorded on BDDE (A) and DP voltammograms of CPD recorded on 3-SP/BDDE (B)in the concentration range 0.025-1.9 µmol L^{-1}, DP and SW voltammograms of FLU recorded on BDDE in the concentration range 2-10 µmol L^{-1} (C), and SW voltammograms of FLU recorded on BDDE in the range 0.25-50 µmol L^{-1} (D).*

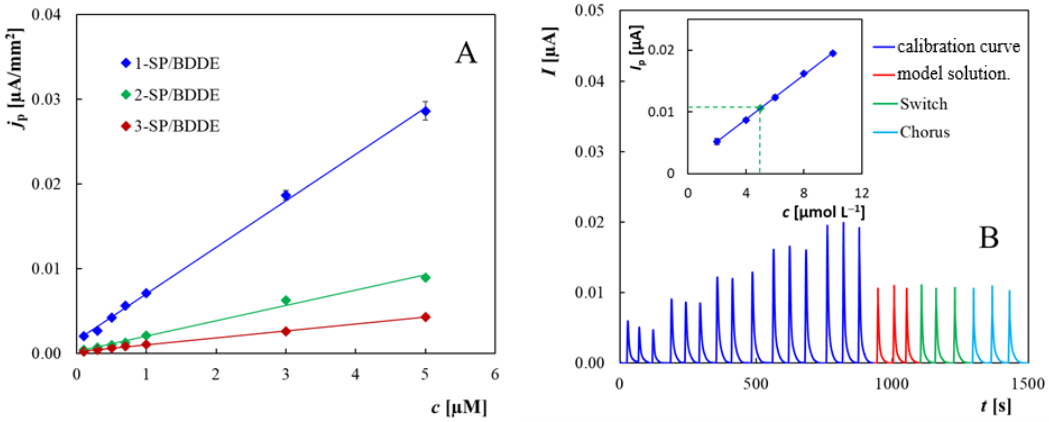

Figure 10: *Dependences of j_p on c_{CPD} recorded using FIA-ED for individual SP/BDDEs (A) and analysis of model solution, Chorus, and Switch using FIA-ED with 1-SP/BDDE.*

3.2.3 Analysis of Model Solutions and Real Samples

All methods and sensors were applied to model solutions and real samples analysis, with results summarized in Tables 4 and 5. An example of analyzes of real samples with CPD

content using FIA-ED is shown in Figure 10B. Enriched natural water with CPD concentration of $5{,}0\times10^{-8}$ mol L^{-1} was analyzed using direct DPV without pre-concentration, while FLU with the concentration of $1{,}0\times10^{-8}$ mol L^{-1} required solid-phase extraction. CPD was also determined in commercial pesticide products, with results compared to HPLC/DAD as a reference method. In conclusion, various electroanalytical methods were developed for CPD and FLU, enabling successful analysis in model solutions and complex matrices, achieving reliable results across different sensor designs.

Table 4: Results of CPD determination in model solutions, spiked river water, and pesticide formulations using all developed methods.

Sample	**Method**	**Electrode**	**Added [nmol L^{-1}]**	**Found [nmol L^{-1}]**	**Recovery [%]**	**RSD_5 [%]**
Model solution	DPV	BDDE	50	50.8±2.0	95.3-104.3	3.9
		1-SP/BDDE		48.5±2.3	94.0-102.4	4.7
		2-SP/BDDE		50.2±1.9	96.3-104.2	3.7
		3-SP/BDDE		50.9±1.9	97.2-106.0	3.8
	FIA-ED	1-SP/BDDE	500	502±13	96.1-104.6	2.7
		2-SP/BDDE		505±15	96.5-105.1	2.9
		3-SP/BDDE		513±17	95.6-106.1	3.7
River water	DPV	BDDE	50	50.2±1.7	96.2-104.7	3.5
		1-SP/BDDE		50.5±1.2	95.8-105.1	3.5
		2-SP/BDDE		49.9±1.3	96.0-104.8	3.4
		3-SP/BDDE		50.1±1.0	96.2-105.9	3.1
			Declared [g kg^{-1}]	Found [g kg^{-1}]		
Chorus	DPV	BDDE	500	502.6±17.9	95.5-105.4	3.6
		1-SP/BDDE		501.5±16.7	96.8-105.8	3.3
		2-SP/BDDE		496.1±11.7	94.5-104.7	3.6
		3-SP/BDDE		503.0±9.13	96.8-103.9	2.7
	FIA-ED	1-SP/BDDE		504.6±10.3	96.5-105.3	3.1
		2-SP/BDDE		498.9±11.0	96.5-105.1	3.3
		3-SP/BDDE		510.5±11.0	96.6-105.0	3.2
	HPLC/DAD	---		502.3±10.8	97.3-105.7	2.3
Switch	DPV	BDDE	375	372.4±11.3	95.6-107.2	4.6
		1-SP/BDDE		376.7±12.1	94.1-104.2	4.8
		2-SP/BDDE		375.8±7.2	96.5-103.6	2.9
		3-SP/BDDE		374.6±7.9	94.4-102.2	3.2
	FIA-ED	1-SP/BDDE		377.0±9.0	96.5-105.3	3.6
		2-SP/BDDE		373.8±10.2	95.6-106.1	4.1
		3-SP/BDDE		380.5±8.7	96.9-106.7	3.4
	HPLC/DAD	---		378.2±7.5	97.0-105.1	3.0

Table 5: Results of FLU determination in model solutions and river water without concentration and after extraction.

Sample	Method	Electrode	Added [µmol L^{-1}]	Found [µmol L^{-1}]	Recovery [%]	RSD_5 [%]
Model Solution	SWV	BDDE	0.25	0.252±0.013	95.0-110.3	5.1
		BDDE	1.0	0.994±0.012	101.5-104.9	1.2
	SWV	1-SP/BDDE	1.0	0.964±0.012	95.6-98.5	1.2
		2-SP/BDDE	1.0	1.001±0.024	96.7-103.3	2.4
		3-SP/BDDE	1.0	0.923±0.022	89.5-95.4	2.4
River Water	SWV_P	BDDE	0.5	0.476±0.020	90.2-102.0	4.2
			1.0	0.970±0.020	93.8-99.6	2.0
	SWV_{SPE}	BDDE	0.01	0.0105±0.00048	95.0-110.3	4.6
			Added [g kg^{-1}]	Found [g kg^{-1}]		
Switch	SWV	BDDE	375	373.6±10.8	96.8-107.1	4.5
		3-SP/BDDE	375	377.1±2.3	97.2-108.3	4.7

SWV_P – direct SWV analysis without pre-concentration, SWV_{SPE} – SWV analysis after solid phase extraction

3.3 Printed Sensors with Structured BDDE Surface

Technological advancements enable the development of new electrode materials and modifications of existing ones. In the past, much attention was also paid to the modification of BDDE. The structured surface of the WE increases the real surface area leading to improved electroanalytical properties, particularly sensitivity and selectivity towards specific analytes, even in the case of BDDE. The preparation method for sensors with a structured BDDE surface (sSP/BDDE) was detailed in the experimental section. The substrate surface was modified with a laser to create grids with defined square dimensions of 15, 20, and 25 µm, with depths varying by repeating laser scans 5× or 10×, resulting in sensors labeled: 5×15, 5×20, 5×25, and 10×15, 10×20, 10×25 µm. BDD was deposited onto the modified substrate, with the working electrode diameter of 3 mm, corresponding to the 3-SP/BDDE sensor. The electrochemical properties of the new sSP/BDDE sensors were studied, focusing on their application for analyzing the pesticide CPD.

3.3.1 Electrochemical Properties of Printed Sensors with Structured BDDE

For the electrochemical characterization of sSP/BDDE, cyclic voltammetry (CV) and electrochemical impedance spectroscopy (EIS) were applied using two redox markers: $[Fe(CN)_6]^{4-/3-}$ and $[Ru(NH_3)_6]^{2+/3+}$. The measured CV for $[Fe(CN)_6]^{4-/3-}$ and $[Ru(NH_3)_6]^{2+/3+}$ (Fig. 11A, B) showed that for the Fe complex, the ratio of the oxidation peak height to the reduction peak height varied between 0.97 and 1.03, indicating a reversible reaction. The potential difference (ΔE_p) for the 5×15 and 10×15 sensors was 100.7 mV, significantly improved compared to 3-SP/BDDE (171.2 mV), indicating accelerated electrode reaction kinetics. However, the 5×20 sensor showed a notable decline in reversibility with ΔE_p reaching 493.5 mV.

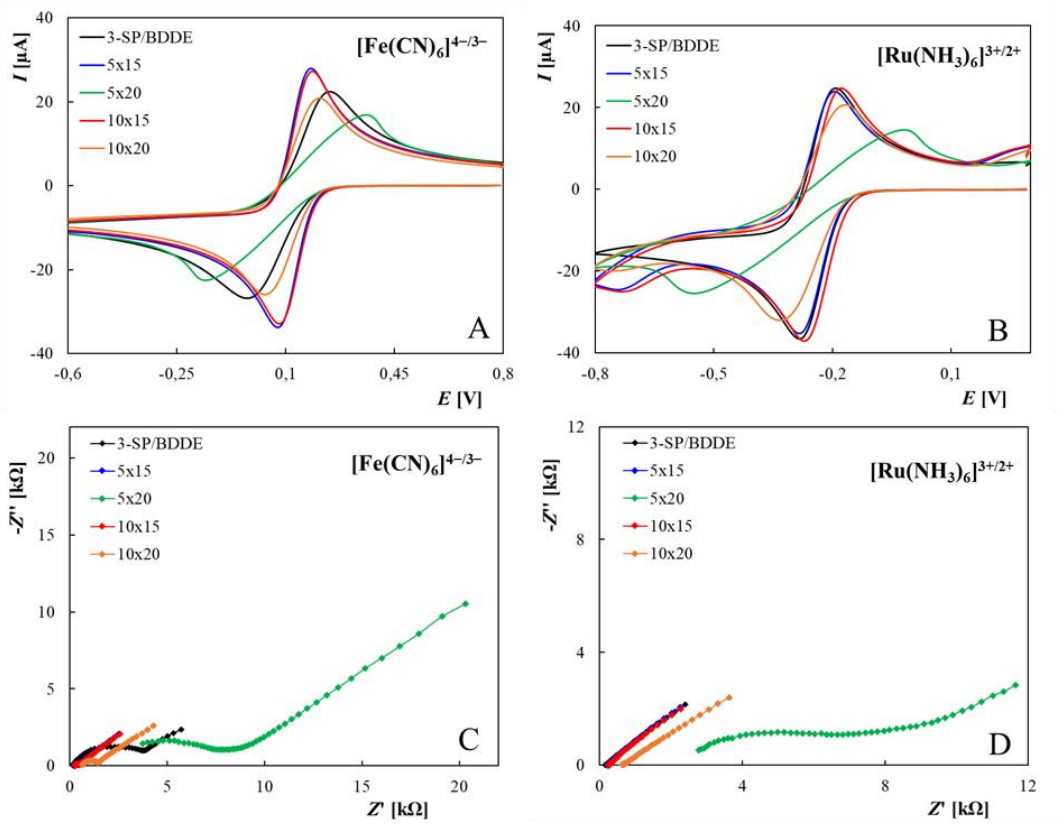

Figure 11: *Cyclic voltammograms of $[Fe(CN)_6]^{4-/3-}$ (A) and $[Ru(NH_3)_6]^{2+/3+}$ (B) and EIS spectra of $[Fe(CN)_6]^{4-/3-}$ (C) and $[Ru(NH_3)_6]^{2+/3+}$ (D) recorded on sSP/BDDE and 3-SP/BDDE.*

EIS was used to further investigate the electrochemical properties of the new structured sensors. The measured spectra correlated well with CV results, showing that sensors with smaller ΔE_p also had lower charge transfer resistance, ranging from 180-200 Ω. The largest resistance (8.5 kΩ) was noted for the 5×20 sensor. The Ru complex exhibited faster kinetics, with only Warburg diffusion observed, while the 5×20 sensor indicated slowed kinetics, confirming the electrochemical property deterioration detected via CV.

In summary, among electrodes treated with the same number of laser scans (5 or 10), increasing the square side length from 15 to 25 µm worsened electrochemical properties. Compared to the unmodified sensor, better results (higher I_p and lower ΔE_p) were only achieved with the smallest structured sensors (5×15 and 10×15). Increasing the square side to 25 µm significantly increased electrical resistance, making those sensors unsuitable for electrochemical applications.

3.3.2 Applications of Printed Sensors with Structured BDDE in Electroanalysis

Using method developed during the optimization of CPD determination, key statistical parameters were established for all tested substances and structured sensors. Concentration dependencies for CPD measured on various sSP/BDDE configurations showed the same linear range as conventional electrodes (Fig. 12). The lowest limit of detection for CPD was achieved with the 10×15 sSP/BDDE configuration, indicating excellent sensitivity. The highest correlation coefficient (r = 0.9994) was recorded for the 5×15 configuration, demonstrating excellent linearity in CPD measurements.

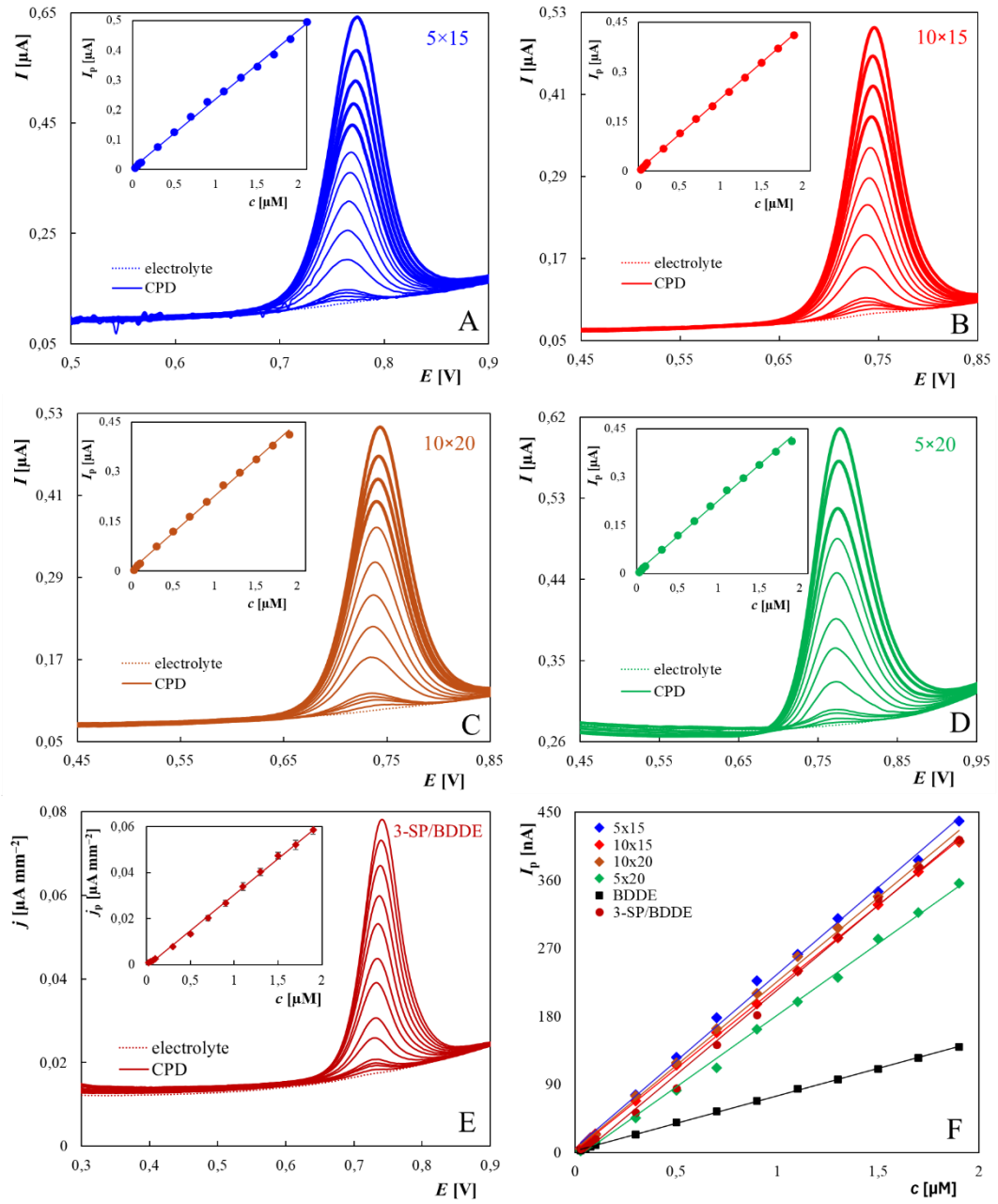

Figure 12: *DP voltammograms of CPD obtained on sSP/BDDE (A-D) and 3-SP/BDDE (E), dependencies of* I_p *on* c_{CPD} *(F).*

In Fig. 12 F, the dependences of I_p on c_{CPD} for all tested sensors are shown, and Table 6 provides an overview of the statistical parameters. The sensitivity of all tested sSP/BDDE was higher than that of 3-SP/BDDE (0.03171±0.00049), which corresponds to the fact that surface modification increased the area of the working electrode (WE). Among the different variants of sSP/BDDE, the slopes of the concentration dependencies were very similar for all sensors (*e.g.*, (0.22935±0.00329) for sSP/BDDE 5×15), with the except of sSP/BDDE 5×20, which exhibited slightly lower sensitivity (0.18947±0.00251). This aligns with the findings of previous studies using CV and EIS, where this sensor displayed the worst electrochemical properties.

Table 6: Statistical parameters of concentration dependences of CPD obtained on all tested sSP/BDDE and 3-SP/BDDE (0.025-1.9 μmol L^{-1}).

Electrode	**Slope** [μA L^{-1}/μmol]	**Intercept** [μA]	***r***
3SP/BDDE	0.03171±0.00049	0.00120±0.00049	0.9984
5×15	0.2294±0.0033	0.00654±0.00332	0.9994
10×15	0.21597±0.00098	0.00313±0.00099	0.9954
10×20	0.2215±0.0029	0.00478±0.00292	0.9948
5×20	0.1895±0.0025	–0.00786±0.00254	0.9851

Conclusion

This dissertation focused primarily on testing the application possibilities of screen-printed sensors with boron-doped diamond working electrodes in electroanalysis. The introductory literature review presents an overview of the most commonly used working electrodes in voltammetry, specifically focusing on printed sensors and their potential applications in the analysis of environmental and biological samples, particularly in the determination of pharmaceuticals and pesticides.

The study of the electrochemical behavior of the drug GFE and the pesticides CPD and FLU using BDDE provided important insights for the development of voltammetric methods for their determination. These methods were subsequently transferred to SP/BDDE while maintaining the optimized parameters of the individual voltammetric techniques. It was found that the tested printed sensors provided lower limits of detection (LOD) and generally wider linear dynamic ranges (LDR) for all analyzed substances than conventional BDDE setups. Additionally, several significant advantages of solid-phase extraction (SPE) were utilized in this work. Firstly, the possibility of analyzing small sample volumes was verified when determining the drug GFE in serum using a 50 μL droplet. Secondly, the ease of incorporating printed sensors into electrochemical detectors for flow analysis was demonstrated. The proposed methods were successfully applied in the analysis of a range of real samples, including commercially available pharmaceutical or pesticide preparations, natural waters, and serum. It was shown that the used sensors with suitably set parameters also allow for the analysis of complex samples with complicated matrices.

Finally, preliminary studies were conducted to test the electrochemical properties of sensors with structured BDDE surfaces. It was found that when comparing electrodes treated with the same number of laser scans (5 or 10), increasing the side length of the square from 15 to 25 μm degraded the electrochemical properties. Increasing the side length to 25 μm resulted in a significant increase in electrical resistance, making the sensors unusable. Compared to 3-SP/BDDE, only the sSP/BDDE with the shortest square sides (5×15 and 10×15) exhibited better electrochemical properties. In the analysis of CPD, all sSP/BDDE were more sensitive than the comparative unmodified 3-SP/BDDE, with the worst sensitivity among the modified sensors being provided by sSP/BDDE 5×20. This confirmed the anticipated positive effect of a larger working electrode area on analysis sensitivity.

The results achieved suggest that printed sensors have the potential to become a useful tool in the rapid and sensitive analysis of environmentally and pharmaceutically significant substances in real samples, not only in laboratory analysis but also as part of flow or field analyzers and point-of-care testing systems.

List of citations

1. J. Jindra, Dějiny Elektrochemie v Českých Zemích 1882-1989, 1. vyd, Libri : Ústav pro soudobé dějiny, (2009) Praha.
2. Elektroanalytická chemie životního prostředí, 1., Praha : Nakladatelství techn. lit., 1985.
3. S.A. Ozkan, Electroanalytical Methods in Pharmaceutical Analysis and Their Validation, HNB Publ, (2012) New York, NY.
4. F. Opekar, Základní analytická chemie pro studenty, pro něž analytická chemie není hlavním studijním oborem, 2. vyd, Karolinum, (2010) Praha.
5. W. Zhang, R. Wang, F. Luo, P. Wang, Z. Lin, *Chinese Chemical Letters*, 31 (2020) 589–600.
6. M. Iwaki, S. Sato, K. Takahashi, H. Sakairi, *Nuclear Instruments and Methods in Physics Research*, 209–210 (1983) 1129–1133.
7. C. Shan, H. Yang, J. Song, D. Han, A. Ivaska, L. Niu, *Anal. Chem.*, 81 (2009) 2378–2382.
8. S. Matsumoto, Y. Sato, M. Kamo, N. Setaka, *Jpn. J. Appl. Phys.*, 21 (1982) L183.
9. M. Kamo, Y. Sato, S. Matsumoto, N. Setaka, *Journal of Crystal Growth*, 62 (1983) 642–644.
10. K. Pecková, J. Musilová, J. Barek, *Crit. Rev. Anal. Chem.*, 39 (2009) 148–172.
11. N. Fujimori, T. Imai, A. Doi, *Vacuum*, 36 (1986) 99–102.
12. M. Marton, M. Vojs, P. Michniak, M. Behúl, V. Rehacek, M. Pifko, Š. Stehlík, A. Kromka, *Diam. Relat. Mater.*, 126 (2022) 109111.
13. T. Kondo, *Curr. Opin. Electrochem.*, 32 (2022) 100891.
14. J. Barek, J. Fischer, T. Navrátil, K. Pecková, B. Yosypchuk, J. Zima, *Electroanalysis*, 19 (2007) 2003–2014.
15. S. Baluchová, A. Taylor, V. Mortet, S. Sedláková, L. Klimša, J. Kopeček, O. Hák, K. Schwarzová-Pecková, *Electrochimica Acta*, 327 (2019) 135025.
16. V. Hrdlička, O. Matvieiev, T. Navrátil, R. Šelešovská, *Electrochim. Acta*, 456 (2023) 142435.
17. A. Salimi, V. Alizadeh, R. Hallaj, *Talanta*, 68 (2006) 1610–1616.
18. A.J. Bard, L.R. Faulkner, Electrochemical Methods: Fundamentals and Applications, 2nd ed, Wiley, (2001) New York.
19. S. Baluchová, K. Schwarzová-Pecková, A. Taylor, S. Sedláková, V. Mortet, L. Klimša, J. Kopeček, Vorträge, AMA Service GmbH, Von-Münchhausen-Str. 49, 31515 Wunstorf, Germany, (2021) Online, pp. 43–46.
20. N.F. Barros Azeredo, M.S. Ferreira Santos, J.R. Sempionatto, J. Wang, L. Angnes, *Anal. Chem.*, 94 (2022) 250–268.
21. S. Đurđić, F. Vlahović, M. Markićević, J. Mutić, D. Manojlović, V. Stanković, Ľ. Švorc, D. Stanković, *Chemosensors*, 11 (2023) 15.
22. O.D. Renedo, M.A. Alonso-Lomillo, M.J.A. Martínez, *Talanta*, 73 (2007) 202–219.
23. W. Lee, H. Koo, J. Sun, J. Noh, K.-S. Kwon, C. Yeom, Y. Choi, K. Chen, A. Javey, G. Cho, *Sci Rep*, 5 (2015) 17707.
24. O. Matvieiev, R. Šelešovská, M. Vojs, M. Marton, P. Michniak, V. Hrdlička, M. Hatala, L. Janíková, J. Chýlková, J. Skopalová, P. Cankař, T. Navrátil, *Biosensors*, 12 (2022) 241.
25. P. Richter, Encyclopedia of Toxicology, Elsevier, (2014), pp. 806–808.
26. H.H. Albrecht, P.V. Dicpinigaitis, E.P. Guenin, *Multidiscip. Respir. Med.*, 12 (2017) 31.
27. G. Wang, F.J. Burczynski, B.B. Hasinoff, K. Zhang, Q. Lu, J.E. Anderson, *Mol. Pharmaceutics*, 6 (2009) 895–904.
28. A. Collaku, Y. Yue, K. Reed, *JPR*, 10 (2017) 669–678.
29. S.S.A. El-Hay, R.E. Sheikh, M. Ali, A.A. Gouda, H.M. El-Sayed, *Talanta*, 8 (2023) 100233.

30. I.A. Naguib, S.A. Farag, H.E. Zaazaa, E.A. Abdelaleem, *J. Chromatogr. Sci.*, 59 (2021) 419–424.
31. S.A. Mousazadeh Hassani, *Chromatographia*, 83 (2020) 791–805.
32. A.S. Fayed, S.A. Boltia, A. Musaed, M.A. Hegazy, *J. Pharm. Biomed. Anal.*, 177 (2020) 112821.
33. A. Nezhadali, M.R. Shapouri, M. Amoli-Diva, A.H. Hooshangi, F. Khodayari, *Heliyon*, 5 (2019) e02871.
34. J. Wen, H. Zhang, C. Xia, X. Hu, W. Xu, X. Cheng, J. Gao, Y. Xiong, *Biomed. Chromatogr.*, 24 (2010) 351–357.
35. O.A. El-Naem, S.S. Saleh, *Microchem. J.*, 166 (2021) 106234.
36. T. Harsono, M. Yuwono, G. Indrayanto, *J. AOAC Int.*, 88 (2005) 1093–1098.
37. M.H.M. Sharaf, D.D. Stiff, *J. Pharm. Biomed. Anal.*, 35 (2004) 801–806.
38. T.T. Brandhorst, B.S. Klein, *Food and Chemical Toxicology*, 123 (2019) 561–565.
39. E. de Nadal, F. Posas, *FEMS Yeast Research*, 22 (2022) foac013.
40. D.A.M. Alexandrino, A.P. Mucha, C.M.R. Almeida, M.F. Carvalho, *Journal of Hazardous Materials*, 394 (2020) 122545.
41. Y. Wang, C. Xu, D. Wang, H. Weng, G. Yang, D. Guo, R. Yu, X. Wang, Q. Wang, *Environmental Pollution*, 260 (2020) 114105.
42. F. Orton, E. Rosivatz, M. Scholze, A. Kortenkamp, *Environmental Health Perspectives*, 119 (2011) 794–800.
43. R. Rial Otero, C. Yagüe Ruiz, B. Cancho Grande, J. Simal Gándara, *J. Chromatogr. A*, 942 (2002) 41–52.
44. X. Liang, X. Liu, F. Dong, J. Xu, D. Qin, Y. Li, Y. Tian, Y. Zhang, Y. Han, Y. Zheng, *Food Additives & Contaminants: Part A*, 30 (2013) 713–721.
45. A.E. Bulgurcuoğlu, B.Y. Durak, D.S. Chormey, S. Bakırdere, *Microchem. J.*, 168 (2021).
46. P. Cabras, A. Angioni, V.L. Garau, E.V. Minelli, *Journal of AOAC INTERNATIONAL*, 80 (1997) 867–870.
47. J.V. Mercader, A. Abad-Fuentes, C. Agulló, A. Abad-Somovilla, F.A. Esteve-Turrillas, *Anal. Methods*, 6 (2014) 8924–8929.
48. M. Brycht, B. Burnat, S. Skrzypek, V. Guzsvány, N. Gutowska, J. Robak, A. Nosal–Wiercińska, *Electrochimica Acta*, 158 (2015) 287–297.
49. F. Waechter, E. Weber, T. Hertner, U. May-Hertl, Hayes' Handbook of Pesticide Toxicology, Elsevier, (2010), pp. 1903–1913.
50. C.-C. Fang, F.-Y. Chen, C.-R. Chen, C.-C. Liu, L.-C. Wong, Y.-W. Liu, J.-G.J. Su, *Toxicology*, 304 (2013) 32–40.
51. O. of P. United States Environmental Protection Agency Pesticides and Toxic SUbstances, (1998).
52. C. Tang, C. Shen, K. Zhu, Y. Zhou, Y.-J. Chuang, C. He, Z. Zuo, *Ecotoxicology and Environmental Safety*, 201 (2020) 110808.
53. C. Tang, Y. Zhu, C. Yang, C. He, Z. Zuo, *Science of The Total Environment*, 846 (2022) 157504.
54. L. Vaquero-Fernández, A. Sáenz-Hernáez, J. Sanz-Asensio, P. Fernández-Zurbano, M. Sainz-Ramírez, B. Pons-Jubera, M. López-Alonso, S. Epifanio-Fernández, M. Martínez-Soria, *J. Sci. Food Agric.*, 88 (2008) 1943–1948.
55. M.S. Munitz, S.L. Resnik, M.I.T. Montti, *Food Additives & Contaminants: Part A*, 30 (2013) 1299–1307.
56. F.A. Esteve-Turrillas, J.V. Mercader, C. Agulló, A. Abad-Somovilla, A. Abad-Fuentes, *Analyst*, 142 (2017) 3975–3985.
57. F.A. Esteve-Turrillas, J.V. Mercader, C. Agulló, A. Abad-Somovilla, A. Abad-Fuentes, *LWT - Food Science and Technology*, 63 (2015) 604–611.
58. E.A. Ayhan, R. İnam, *Food Measure*, 14 (2020) 1333–1343.

List of Student´s Published Works

Articles on the topic of the dissertation theses

Kelíšková P., Matvieiev O., Janíková L., Šelešovská R.: *Recent advances in the use of screen-printed electrodes in drug analysis: A review*. Current Opinion in Electrochemistry 42, 101408 (2023). ISSN 2451-9103. DOI: 10.1016/ j.coelec.2023.101408

Kelíšková P., Matvieiev O., Jiroušková E., Sokolová R., Janíková L., Behúl M., Šelešovská R.: *Voltammetric and flow amperometric determination of drug guaifenesin in pharmaceutical and biological samples using screen-printed sensor with boron doped diamond electrode.* Talanta 281, 126809 (2025). DOI10.1016/j.talanta.2024.126809

Next articles

Šelešovská R., **Martinková P.**, Štěpánková M., Navrátil T., Chýlková J.: Comparison study of voltammetric behavior of muscle relaxant dantrolene sodium on silver solid amalgam and bismuth film electrodes. J. Anal. Meth. Chem. 2017, ID 3627428, 12 pages (2017). DOI 10.1155/2017/3627428

Šelešovská, R., Kränková, B., Štěpánková, M., **Martinková, P.**, Janíková, L., Chýlková, J., & Vojs, M.: *Influence of boron content on electrochemical properties of boron-doped diamond electrodes and their utilization for leucovorin determination*. Journal of Electroanalytical Chemistry. Vol. 821, Pages 2-9, (2018)

Šelešovská, R., Kränková, B., Štěpánková, M., **Martinková, P.**, Janíková, L., Chýlková, J., & Navrátil, T. (2018). Voltammetric determination of leucovorin in pharmaceutical preparations using a boron-doped diamond electrode. *Monatshefte für Chemie-Chemical Monthly, 149*, 1701-1708.

Štěpánková, M., Šelešovská, R., Janíková, L., **Martinková, P.**, Marton, M., Michniak, P., & Chýlková, J. (2018). Porovnání borem dopovaných diamantových elektrod s různým obsahem boru při stanovení herbicidu linuronu a léčiva mesalazinu. *Chemické listy, 112*(6), 389-395.

Šelešovská, R., Herynková, M., Skopalová, J., **Kelíšková-Martinková, P.**, Janíková, L., & Chýlková, J. (2019). Reduction behavior of insecticide azoxystrobin and its voltammetric determination using silver solid amalgam electrode. *Monatshefte für Chemie-Chemical Monthly, 150*, 419-428. DOI: 10.1007/s00706-018-2348-y

Šelešovská, R., Herynková, M., Skopalová, J., **Kelíšková-Martinková, P.**, Janíková, L., Cankař, P., ... & Chýlková, J. (2019). Oxidation Behavior of Insecticide Azoxystrobin and its Voltammetric Determination Using Boron-doped Diamond Electrode. *Electroanalysis, 31*(2), 363-373. DOI: 10.1002/elan.201800647

Šelešovská, R., Schwarzová-Pecková, K., Sokolová, R., Krejčová, K., & **Martinková-Kelíšková, P.** (2021). The first study of triazole fungicide difenoconazole oxidation and its voltammetric and flow amperometric detection on boron doped diamond electrode. *Electrochimica Acta, 381*, 138260. DOI: 10.1016/j.electacta.2021.138260